

Geodinamica Acta

ISSN: 0985-3111 (Print) 1778-3593 (Online) Journal homepage: https://www.tandfonline.com/loi/tgda20

The Manyas fault zone (southern Marmara region, NW Turkey): active tectonics and paleoseismology

Akın Kürçer, Volkan Özaksoy, Selim Özalp, Çağıl Uygun Güldoğan, Ersin Özdemir & Tamer Y. Duman

To cite this article: Akın Kürçer, Volkan Özaksoy, Selim Özalp, Çağıl Uygun Güldoğan, Ersin Özdemir & Tamer Y. Duman (2017) The Manyas fault zone (southern Marmara region, NW Turkey): active tectonics and paleoseismology, Geodinamica Acta, 29:1, 42-61, DOI: 10.1080/09853111.2017.1294013

To link to this article: https://doi.org/10.1080/09853111.2017.1294013

© 2017 The Author(s). Published by Informa UK Limited, trading as Taylor & Francis Group

Published online: 28 Feb 2017.

Submit your article to this journal

Article views: 992

View related articles

View Crossmark data

Citing articles: 1 View citing articles

Full Terms & Conditions of access and use can be found at
https://www.tandfonline.com/action/journalInformation?journalCode=tgda21

Geodinamica Acta, 2017
Vol. 29, No. 1, 42–61, https://doi.org/10.1080/09853111.2017.1294013

Taylor & Francis
Taylor & Francis Group
Check for updates

The Manyas fault zone (southern Marmara region, NW Turkey): active tectonics and paleoseismology

Akın Kürçer[a]*, Volkan Özaksoy[b], Selim Özalp[a], Çağıl Uygun Güldoğan[a], Ersin Özdemir[a] and Tamer Y. Duman[a]

[a]*Department of Geological Research, General Directorate of Mineral Research and Exploration, Çankaya 06800, Ankara, Turkey;* [b]*Department of Marine and Environmental Research, General Directorate of Mineral Research and Exploration, Çankaya 06800, Ankara, Turkey*

(*Received 16 November 2015; accepted 8 February 2017*)

The Manyas fault zone (MFZ) is a splay fault of the Yenice Gönen Fault, which is located on the southern branch of the North Anatolian Fault System. The MFZ is a 38 km long, WNW–ESE-trending and normal fault zone comprised of three en-echelon segments. On 6 October 1964, an earthquake (Ms = 6.9) occurred on the Salur segment. In this study, paleoseismic trench studies were performed along the Salur segment. Based on these paleoseismic trench studies, at least three earthquakes resulting in a surface rupture within the last 4000 years, including the 1964 earthquake have been identified and dated. The penultimate event can be correlated with the AD 1323 earthquake. There is no archaeological and/or historical record that can be associated with the oldest earthquake dated between BP 3800 ± 600 and BP 2300 ± 200 years. Additionally, the trench study performed to the north of the Salur segment demonstrates paleoliquefaction structures crossing each other. The surface deformation that occurred during the 1964 earthquake is determined primarily to be the consequence of liquefaction. According to the fault plane slip data, the MFZ is a purely normal fault demonstrating a listric geometry with a dip of 64°–74° to the NNE.

Keywords: NW Anatolia; southern Marmara; Manyas fault zone; Manyas earthquake; paleoseismology

1. Introduction

On 6 October 1964 an earthquake (Ms = 6.9) hit the southern Marmara Region along the Manyas fault zone (MFZ), and 73 people were killed (Erentöz & Kurtman, 1964; Ketin, 1969; McKenzie, 1972). The earthquake was felt in northwestern Turkey, north of Greece, Bulgaria and the Aegean Islands (Ambraseys, 1988). A foreshock with Ms = 5.0 was observed and 797 aftershocks occurred until 22 October 1964 (Öcal, Üçer, & ve Taner, 1968).

The Manyas earthquake caused extensive liquefaction and lateral spreading around the Salur, Hamamlı, Yeniköy and Kızılköy villages to the south of Lake Manyas. There are different interpretations of the origin of the surface deformation and the seismotectonic features of the earthquake.

The first macro seismic study on the Manyas earthquake was performed by Erentöz and Kurtman (1964). They observed a series of fractures in the Gönen plain, in the area south of Lake Manyas and in the vicinity of the towns Susurluk, Mustafakemalpaşa and Karacabey. These fractures were up to 200 cm long and 5–10 cm wide and indicate that the surface deformation might have occurred due to liquefaction and/or lateral spreading (Erentöz & Kurtman, 1964). The strike of the fractures were reported as N–S in the Gönen plain, E–W in the area south of Lake Manyas, N–S to NNW–SSE partly and WNW–ESE in the Susurluk region and E–W in the regions of Mustafakemalpaşa and Karacabey. Erentöz and Kurtman (1964) stated that during the Manyas earthquake although the northern coastal plain of Lake Manyas was stable, the southern part of the lake subsided. According to Erentöz and Kurtman (1964), the source of earthquake was likely located along E–W-trending faults.

Another macro seismic study on the Manyas earthquake was carried out by Ketin (1969), who mapped a series of NW-trending en-echelon fractures in the vicinity of the villages of Hamamlı, Salur, Kızılköy and Yeniköy. These fractures were interpreted as tension cracks that developed as a result of dextral strike-slip faulting (Ketin, 1969).

There are many different seismological results associated with the source parameters of Manyas earthquake. The first seismological study, which was performed by Canıtez (1968), stated that the vertical component was much larger than the horizontal component associated with the Manyas earthquake. Another seismological study was performed by Öcal et al. (1968) whose focal mechanism solution shows that the Manyas earthquake originated from a WNW-trending reverse fault. According to Öcal et al. (1968) the coordinates of the epicentre were 40.10° N, 27.90° E (south of the MFZ), with a focal depth of 24 km. According to the focal mechanism solution of McKenzie (1972), however the 1964 earthquake originated along a NW-trending normal fault with epicentral coordinates of 40.30° N, 28.23° E (NE of

*Corresponding author. Email: akin.kurcer@mta.gov.tr

© 2017 The Author(s). Published by Informa UK Limited, trading as Taylor & Francis Group.
This is an Open Access article distributed under the terms of the Creative Commons Attribution License (http://creativecommons.org/licenses/by/4.0/), which permits unrestricted use, distribution, and reproduction in any medium, provided the original work is properly cited.

Lake Manyas) and 10–24 km for the focal depth. Kıyak (1986) suggested that the coordinates of the epicentre were 40.18° N, 28.12° E (NE of Lake Manyas) and that the earthquake was sourced by an oblique-slip normal fault. Taymaz, Jackson, and McKenzie (1991) indicated that the Manyas earthquake originated from WNW-trending normal fault and that the coordinates of the epicentre were 40.30° N, 28.23° E (NE of Lake Manyas), with a focal depth of 14 ± 2 km. These differences are primarily associated with the use of different crustal models, initial depths for the moment tensor solutions and the scarcity of avaliable seismological stations.

The structural features and the fault type within the MFZ are controversial in the literature. Şaroğlu, Emre, and Boray (1987) defined the Manyas Fault as an approximately 70-km-long, dextral strike-slip fault extending between the towns of Gönen and Mustafakemalpaşa.

Emre, Doğan, Özalp, and Yıldırım (2011) and Emre et al. (2013) described the MFZ as a 38-km- long, dextral strike-slip fault zone also extending between the towns of Gönen and Mustafakemalpaşa and identified a 16-km-long Salur segment that generated a surface rupture during the 1964 Manyas earthquake. Although the MFZ was defined based on its morphological properties, none of those studies presented fault plane slip data.

In this study, we aim to determine the structural and paleoseismological features of the MFZ and identification of the surface deformation structures.

2. Tectonic setting and regional geology

2.1. *Tectonic setting*

The active tectonics of the Eastern Mediterranean Region is controlled by the North Anatolian fault system (NAFS), East Anatolian fault system (EAFS), Dead sea fault zone (DSFZ) and the Aegean and Cyprean subduction zones. Four main neotectonic provinces developed within the Anatolian Block are separated from each other by these active tectonic structures (Armijo, Meyer,

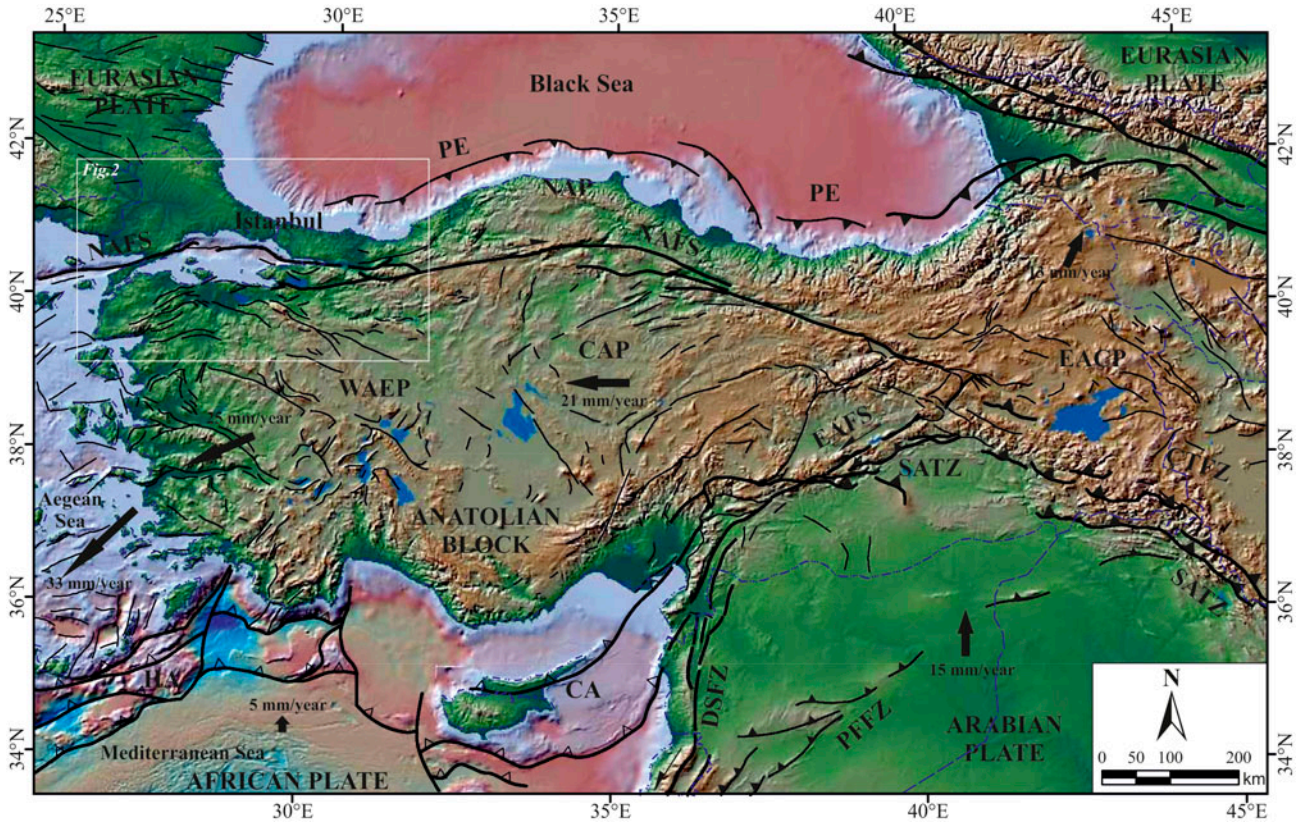

Figure 1. Simplified active fault map of the Eastern Mediterranean region superimposed on topography.
Faults in Turkey are simplified from Emre et al. (2013). Faults the surroundings are from Duman et al. (2016) and references therein. Neotectonic Provence from Şengör et al. (1985). Black arrows and corresponding numbers show GPS-derived plate velocities (mm/year) (Reilinger et al., 2006). Subduction zones are shown by heavy lines with open triangles: the tips of triangles indicate polarity. Heavy lines with filled triangles at hanging wall indicate thrust zones. Heavy lines with half arrows are transform faults: the half arrows show relative movement along these faults. Lines with open triangles represent reverse fault zones. AA Aegean arc, CA Cyprian arc, DSFZ Dead Sea fault zone, EAFZ East Anatolian fault zone, NAFZ North Anatolian fault zone, SATZ Southeast Anatolian Thrust Zone, PE Pontic Escarpment, LC Lesser Caucasus, GC Great Caucasus, WEAP West Anatolian Extensional Provence, CAP Central Anatolian Provence, EACP East Anatolian Compressional Provence, NAP North Anatolian Provence, PFFZ Palmyra fault and Fold Zone. GeoMap Application data were used for the digital elevation model.

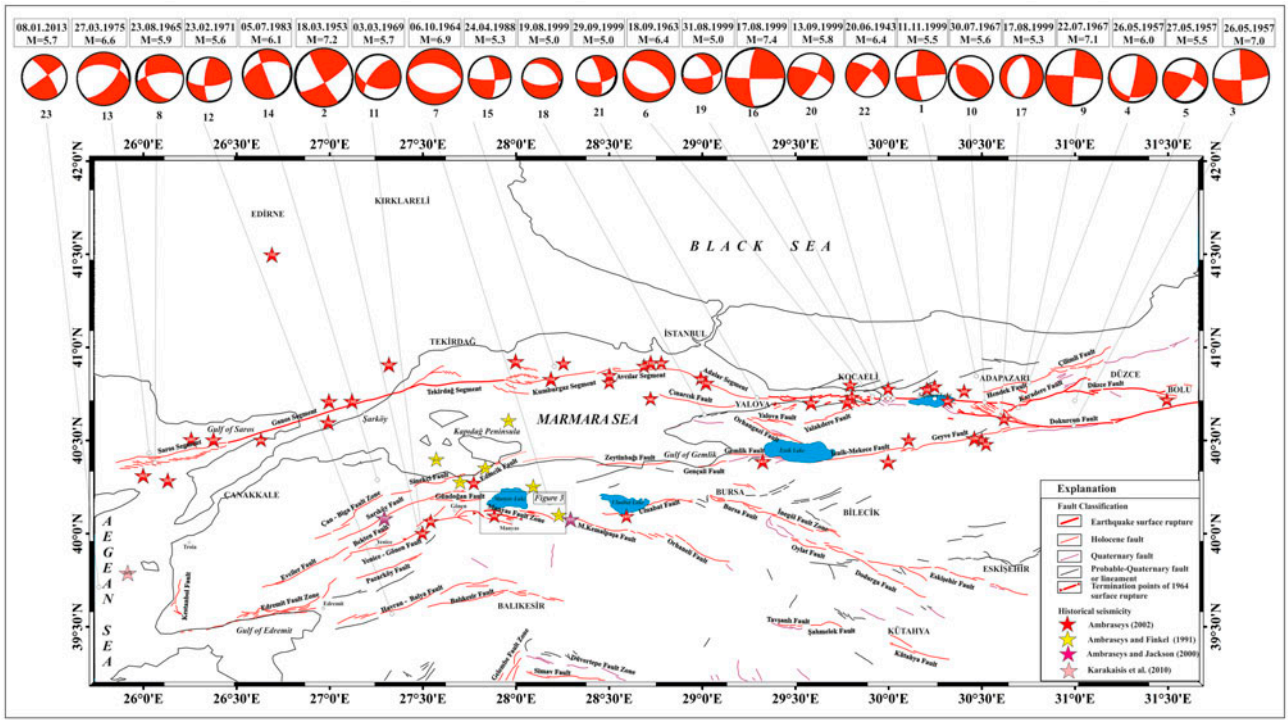

Figure 2. Seismotectonic map of northwestern Turkey.
Active and seismically capable faults were compiled from Emre et al. (2013) and the references include therein. For the references of historical and instrumental earthquakes and focal mecanism solutions see Tables 1 and 2, respectively.

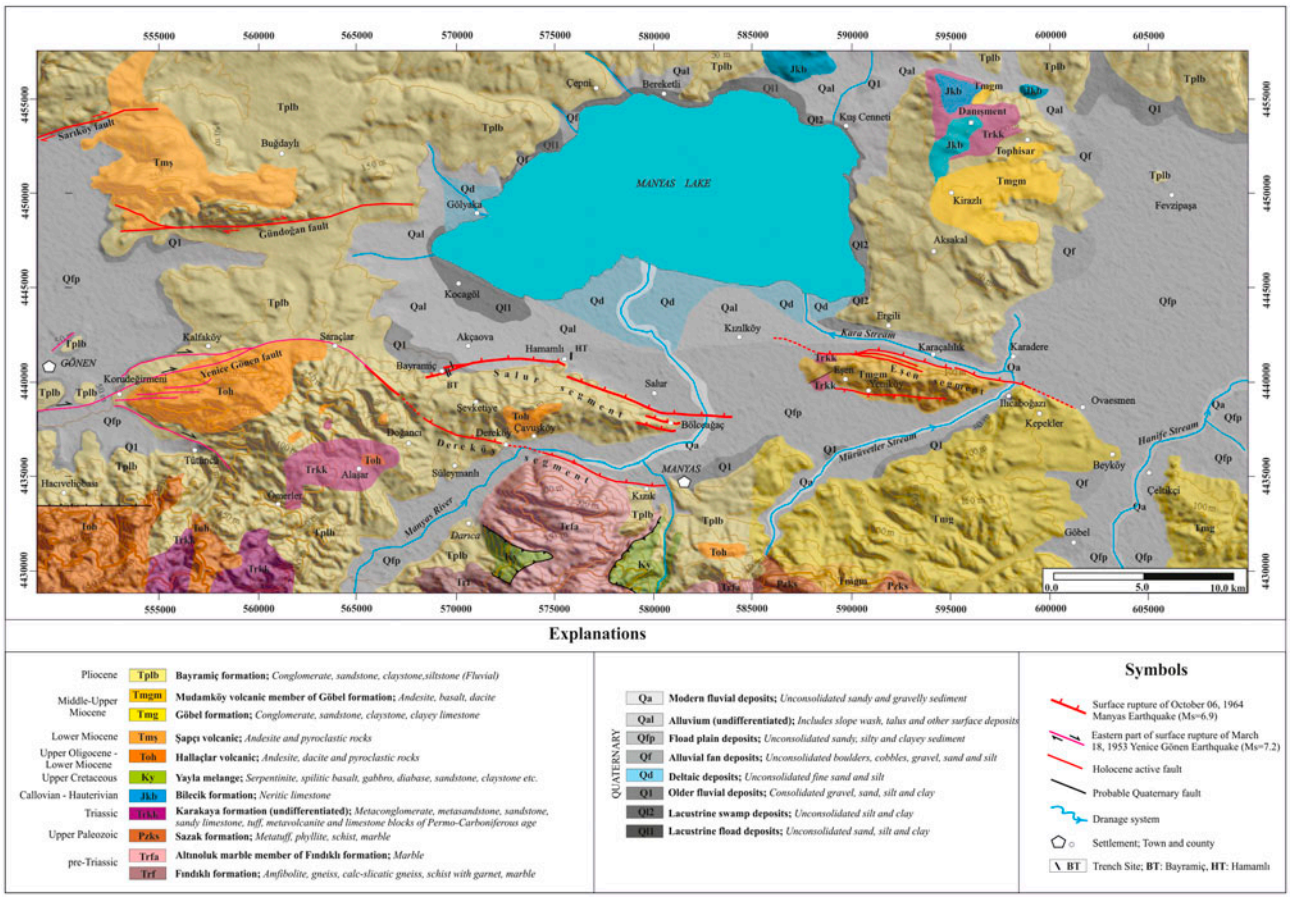

Figure 3. Geological map of the Manyas Fault Zone and its surroundings (pre-Quaternary units are modified from Akçay, Dönmez, Ilgar, Duru, & Pehlivan, 2008; Pehlivan et al., 2011; Quaternary units are modified from Emre, Kazancı, Erkal, Karabıyıkoğlu, & Kuşçu, 1997).

Hubert-Ferrari, & Barka, 1999; Bozkurt, 2001; Jackson & McKenzie, 1984; Le Pichon, Chamot-Rooke, Lallemant, Noomen, & Veis, 1995; McKenzie, 1972, 1978; 1980; Şengör, 1979; Şengör, Görür, & Şaroğlu, 1985; Taymaz et al., 1991) (Figure 1).

The NAFS is seismologically one of the most active fault systems in the Eastern Mediterranean Region. It begins at the Karlıova Triple Junction and extends to the east of Adapazarı. The NAFS bifurcates into two main branches at the east of Adapazarı as northern and southern branches and forms a large-scale horse tail structure (Barka, 1992; Barka & Gülen, 1988) (Figure 1).

The southern branch of the NAFS extends between the east of Adapazarı and Gemlik Gulf. This branch, which extends parallel to the southern shoreline of the Marmara Sea from the Gemlik Gulf to the Kapıdağ Peninsula, forms a restraining bend towards the southwest. This branch is represented by numerous dextral strike-slip faults such as the Edincik Fault, Sarıköy Fault, Yenice Gönen Fault and Edremit Fault Zone in a wide deformation zone between the Kapıdağ Peninsula and Gulf of Edremit (Figure 2).

Recent GPS studies demonstrate that plate motions in and around the Marmara Region are principally accommodated by the northern branch of the NAFS, the data for which suggest a velocity of 24 ± 1 mm/year along this branch (McClusky, Reilinger, Mahmoud, Ben Sari, & Tealeb, 2003; Reilinger et al., 2006). The northern branch of the NAFS facilitates approximately four times as much right-lateral motion (~24 mm/year) as the southern branch does (Meade et al., 2002). In the Southern Marmara Region where the NAFS bifurcates into fault segments across a wide zone, the faults are suggested as dextral with extensional slip rates as varying from 0.9–6.8 mm/year to 0.8–5.5 mm/year (Aktuğ et al., 2009; Ergintav et al., 2014; Flerit, Armijo, King, & Meyer, 2004; Meade et al., 2002; Reilinger et al., 2006).

2.2. *Regional geology*

The basement rocks in the region are composed of Kazdağ metamorphics and the Kalabak Group. Kazdağ metamorphics consist of the pre-Triassic Fındıklı formation (Trf) and Altınoluk marble member (Trfa). These units are tec-



Figure 4. (a) Simplified active fault map of Northwest Turkey (Emre et al., 2013).
Abbreviations: KEF, Kestanbol fault; EFZ, Edremit fault zone; HBFZ, Havran-Balıkesir fault zone; PF, Pazarköy fault; EF, Evciler fault; YGF, Yenice–Gönen fault; MFZ, Manyas fault zone; BF, Bekten fault; ATF, Atıcıoba fault; GÜF, Gündoğan fault; SF, Sarıköy fault; ÇBZ, Çan Biga fault zone; SNF, Sinekçi fault; EDF, Edincik fault; BF, Bandırma fault; MF, Mustafa Kemalpaşa fault; UF, Uluabat fault; BUF, Bursa fault; İFZ, İnagöl fault zone; ZF, Zeytinbağı fault; GF, Gençali fault; GMF, Gemlik fault; ORF, Orhangazi fault; SS, Saros Segment; GS, Gaziköy Segment; TS, Tekirdağ Segment; KS, Kumburgaz Segment; AS, Avcılar Segment; ADS, Adalar Segment; DS, Darıca Segment; KRS, Karamürsel Segment of Northern Branch of North Anatolian fault system (b) Strain ellipsoid for a dextral strike-slip fault, the positions of the Φ_1, Φ_2 and Φ_3 axes of stress as well as the Principle deformation zone (PDZ), P and R synthetic shear and P′ and R′ antithetic shear orientations (modified from Sylvester, 1988).

tonically overlain by the Upper Paleozoic Sazak formation (Pzks) of the Kalabak Group (Duru, Pehlivan, Okay, Şentürk, & Kar, 2012). These metamorphic units are well exposed to the southeast of Manyas and belong to the Sakarya Zone but unconformably overlain by the Karakaya Complex (Trkk) (Figure 3). The Karakaya Complex consists of metaconglomerate, metasandstone, sandy limestone, tuff, metavolcanite and limestone blocks of Devonian – Permian ages (Duru et al., 2012). These units are well exposed to the west of Manyas and the village of Eşen (Figure 3). It is unconformably overlain by Callovian-Hauterivian Bilecik limestone (Jkb). The basement units are tectonically overlain by the Upper Cretaceous Yayla Melange (Ky) (Figure 3).

Basement units are cut by Upper Oligocene – Lower Miocene Hallaçlar Volcanics (Toh), which comprise andesite, dacite and pyroclastic rocks. This formation is comformably overlain by Lower Miocene Şapçı Volcanics (Tmş), which is represented by white tuff and by acidic and andesitic lavas (Genç et al., 2012).

The Hallaçlar Volcanics are unconformably overlain by the Middle-Upper Miocene Göbel Formation (Tmg) and the Mudamköy Volcanic member of this formation (Pehlivan, Duru, Kanar, & Kandemir, 2011). The Göbel

Table 1. Large historical earthquakes occurred in the northwest Turkey.

Date	Latitude°(*N*)	Longitude°(*E*)	Magnitude (*M*)	Location	References
?.?.32	40.5	30.5	7.0	Nicaea (İznik)	Ambraseys (2002)
?.?.68	40.7	30.0	7.2	Nicaea (İznik)	Ambraseys (2002)
?.?.121	40.5	30.1	7.4	Nicomedia (İzmit)	Ambraseys (2002)
10.11.123	40.3	27.7	7.0	Cyzicus (Erdek)	Ambraseys (2002)
?.?.155				Hellespont and Bithynia	Ambraseys and Finkel (1991)
?.?.160	40.0	27.5	7.1	Hellespont (Ç.Boğazı)	Ambraseys (2002)
03.05.180	40.6	30.6	7.3	Nicomedia (İzmit)	Ambraseys (2002)
?.?.268	40.7	29.9	7.3	Nicomedia (İzmit)	Ambraseys (2002)
24.08.358	40.7	30.2	7.4	İzmit	Ambraseys (2002)
02.12.362	40.7	30.2	6.8	İzmit	Ambraseys (2002)
11.10.368	40.5	30.5	6.8	Persis	Ambraseys (2002)
?.11.368	40.1	27.8	6.8	Germe	Ambraseys (2002)
01.04.407	40.9	28.7	6.8	Hebdomon (Bakırköy)	Ambraseys (2002)
25.09.437	40.8	28.5	6.8	İstanbul	Ambraseys (2002)
06.11.447	40.7	30.3	7.2	Nicomedia (İzmit)	Ambraseys (2002)
07.04.460				Cyzicus (Erdek)	Ambraseys and Finkel (1991)
25.09.478	40.7	29.8	7.3	Helenopolis	Ambraseys (2002)
?.?.484	40.5	26.6	7.2	Callipolis	Ambraseys (2002)
06.09.543				Cyzicus (Erdek)	Ambraseys and Finkel (1991)
16.08.554	40.7	29.8	6.9	Nicomedia (İzmit)	Ambraseys (2002)
14.12.557	40.9	28.3	6.9	Silivri	Ambraseys (2002)
26.10.740	40.7	28.7	7.1	Marmara	Ambraseys (2002)
23.05.860	40.8	28.5	6.8	Marmara	Ambraseys (2002)
09.01.869	40.8	29.0	7.0	CP	Ambraseys (2002)
02.09.967	40.7	31.5	7.2	Bolu	Ambraseys (2002)
25.10.989	40.8	28.7	7.2	Marmara	Ambraseys (2002)
23.09.1063	40.8	27.4	7.4	Panio	Ambraseys (2002)
?.09.1065	40.4	30.0	6.8	Nicaea (İznik)	Ambraseys (2002)
01.06.1296	40.5	30.5	7.0	Bithynia	Ambraseys (2002)
?.?.1323				İstanbul	Ambraseys and Finkel (1991)
18.10.1343	40.7	27.1	6.9	Ganos	Ambraseys (2002)
18.10.1343	40.9	28.0	7.0	Heraclea	Ambraseys (2002)
01.03.1354	40.7	27.0	7.4	Hexamili	Ambraseys (2002)
15.03.1419	40.4	29.3	7.2	Bursa	Ambraseys (2002)
10.09.1509	40.9	28.7	7.2	CP	Ambraseys (2002)
10.05.1556				Sea of Marmara	Ambraseys and Finkel (1991)
18.05.1625	40.3	26.0	7.1	Saros	Ambraseys (2002)
17.02.1659	40.5	26.4	7.2	Saros	Ambraseys (2002)
14.02.1672	39.7	25.8	7.0	Bozcaada	Karakaisis et al. (2010)
25.05.1719	40.7	29.8	7.4	İzmit	Ambraseys (2002)
06.03.1737	40.1	27.3	7.0	Aşağı İnova	Ambraseys and Jackson (2000)
29.07.1752	41.5	26.7	6.8	Edirne	Ambraseys (2002)
02.09.1754	40.8	29.2	6.8	İzmit	Ambraseys (2002)
22.05.1766	40.8	29.0	7.1	Marmara	Ambraseys (2002)
05.08.1766	40.6	27.0	7.4	Ganos	Ambraseys (2002)
19.04.1850	40.1	28.3	6.1	Between Manyas & Ulubat Lake	Ambraseys and Jackson (2000)
28.02.1855	40.1	28.6	7.1	Bursa	Ambraseys (2002)
21.08.1859	40.3	26.1	6.8	Saros	Ambraseys (2002)
09.02.1893	40.5	26.2	6.9	Saros	Ambraseys (2002)

Table 2. Parameters and sources for fault plane solutions depicted in Figure 2 (modified from Şengör et al., 2004).

No.	Date (day. month. year)	Origin time (h:min) GMT	Latitude° (*N*)	Longitude° (*E*)	Magnitude	Depth (km)	Strike (°)	Dip (°)	Rake (°)	Reference
1	20.06.1943	15:33	40.83	30.48	6.4	?	176	76	0	McKenzie (1972)
2	18.03.1953	19:06	40.01	27.49	7.2	10*	59	84	14	McKenzie (1972), Ayhan et al. (1981)*
3	26.05.1957	06:33	40.58	31.00	7.0	?	87	78	179	McKenzie (1972)
4	26.05.1957	09:36	40.80	30.80	6.0	?	114	24	−166	Canıtez and Üçer (1967)
5	27.05.1957	11:01	40.70	31.00	5.5	?	293	74	157	Canıtez and Üçer (1967)
6	18.09.1963	16:58	40.71	29.09	6.4	15	304	56	−82	Taymaz et al. (1991)
7	06.10.1964	14:31	40.20	28.20	6.9	14	100	40	−90	Taymaz et al. (1991)
8	23.08.1965	14:08	40.39	26.12	5.9	33	261	70	−132	Kocaefe and Ataman (1976)
9	22.07.1967	16:56	40.67	30.69	7.1	12	275	88	−178	Taymaz et al. (1991)
10	30.07.1967	01:32	40.72	30.52	5.6	16	301	50	70	McKenzie (1972)
11	03.03.1969	00:59	40.08	27.50	5.7	4	219	65	45	McKenzie (1972)
12	23.02.1971	19:41	39.62	27.32	5.6	10	86	66	160	Papadopoulos et al. (1986)
13	27.03.1975	05:15	40.45	26.12	6.6	15	279	46	−43	Jackson and McKenzie (1984)
14	05.07.1983	23:02	40.33	27.21	6.1	15	254	49	−173	GCMT Cataloque
15	24.04.1988	20:49	40.88	28.24	5.3	15	356	71	−11	GCMT Cataloque
16	17.08.1999	00:01	40.70	29.99	7.4	9	91	87	164	GCMT Cataloque
17	17.08.1999	03:14	40.59	30.62	5.3	8	192	32	−82	Örgülü and Aktar (2001)
18	19.08.1999	15:17	40.65	29.09	5.0	4	92	60	−110	Örgülü and Aktar (2001)
19	31.08.1999	08:10	40.74	29.99	5.0	8.6	80	70	−143	Özalaybey et al. (2002)
20	13.09.1999	11:55	40.76	30.07	5.8	12	293	73	164	Örgülü and Aktar (2001)
21	29.09.1999	00:13	40.71	29.30	5.0	8	85	63	−161	Örgülü and Aktar (2001)
22	11.11.1999	14:41	40.78	30.29	5.5	20	307	66	179	Örgülü and Aktar (2001)
23	08.01.2013	14:16	39.65	25.50	5.7	8	54	89	−166	Kürçer, Yalçın, Gülen, and Kalafat (2015)

Table 3. Radiocarbon dating results of samples recovered from Bayramiç Trench 1.

Trench and Wall	Sample no.	Laboratory No (BETA)	Stratigraphic Unit	Sample Material	Measured Radiocarbon Age (BP)	^{13}C / ^{12}C (‰)	Conventional Radiocarbon Age (BP)	Calibrated Age Range (2σ)
Bayramiç 1 – West	BYR.2014/ CW.03	390658	10b	Organic sediment	940 ± 30	−22.7	980 ± 30	Cal AD 1015 to 1050 (Cal BP 935 to 900) and Cal AD 1080 to 1150 (Cal BP 870 to 800)
Bayramiç 1 - West	BYR.2014/ CW.04	390659	11	Organic sediment	320 ± 30	−25.3	320 ± 30	Cal AD 1470 to 1650 (Cal BP 480 to 300)
Bayramiç 1 - West	BYR.2014/ CW.07	390661	10b	Charred material	990 ± 30	−24.8	990 ± 30	Cal AD 995 to 1050 (Cal BP 955 to 900) and Cal AD 1085 to 1125 (Cal BP 865 to 825) and Cal AD 1140 to 1150 (Cal BP 810 to 800)
Bayramiç 1 - West	BYR.2014/ CW.08	390662	10b	Charred material	860 ± 30	−26.3	840 ± 30	Cal AD 1155 to 1260 (Cal BP 795 to 690)
Bayramiç 1 - West	BYR.2014/ CW.09	390663	10b	Charred material	800 ± 30	−23.7	820 ± 30	Cal AD 1165 to 1265 (Cal BP 785 to 685)
Bayramiç 1 - East	BYR.2014/ CE.02	390657	10a	bone	1510 ± 30	−26.6	1650 ± 30	Cal AD 340 to 425 (Cal BP 1610 to 1525)

Table 4. Optically stimulated luminescence (OSL) and Thermo luminescence (TL) dating results of samples recovered from Bayramiç Trench 1.

Trench wall	Sample no.	Stratigraphic unit	Sample material	Equivalent dose (Gy)	Measured OSL age (BP)
Bayramiç 1 West	BYR.2014/OW.01	2	Sand	70.4 ± 8.3	19100 ± 250
Bayramiç 1 West	BYR.2014/OW.02	6	Sand	15.2 ± 2.3	3800 ± 600
Bayramiç 1 West	BYR.2014/CW.05	10a	Ceramic	7.1 ± 0.1	2300 ± 200
Bayramiç 1 East	BYR.2014/CE.02	10a	Ceramic	13.2± 0.9	2900 ± 200

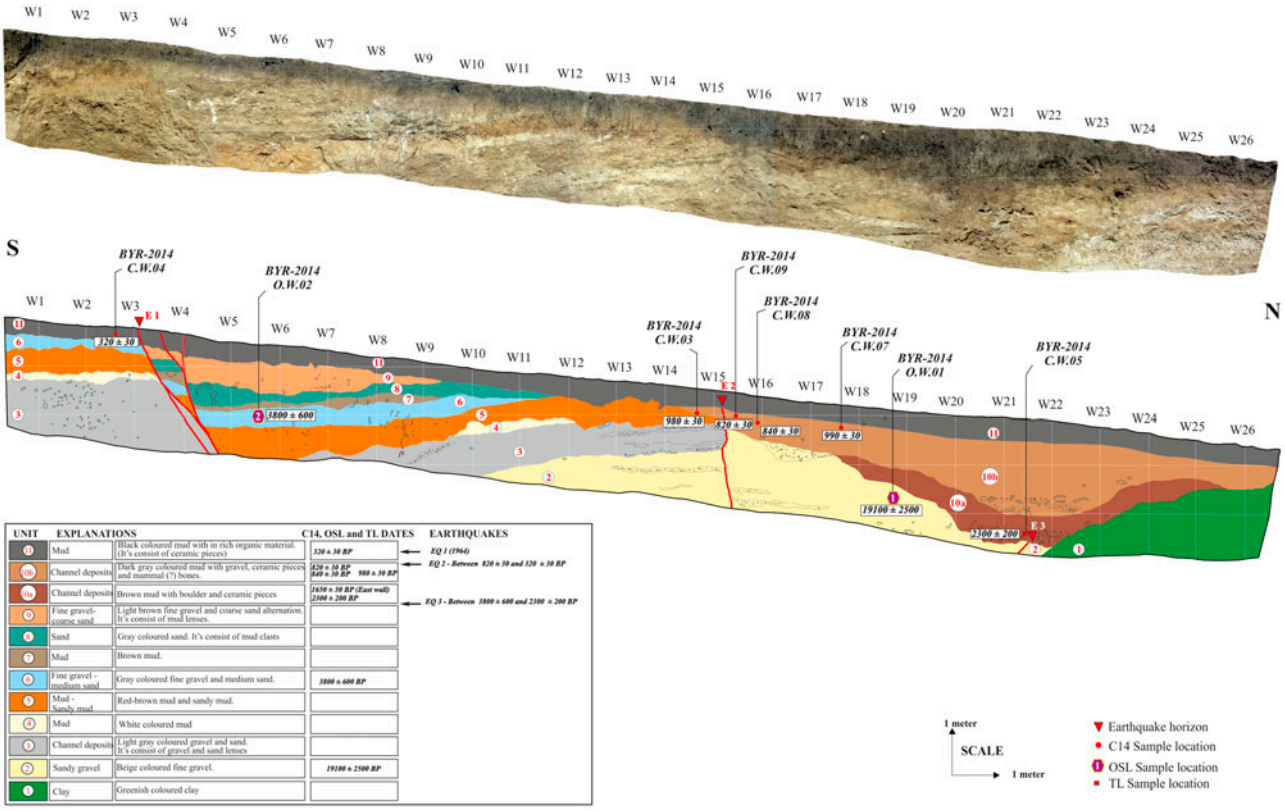

Figure 5. (a) Photomosaic of the Bayramiç Trench 1 western wall without interpretation and (b) Log of the Bayramiç Trench 1 western wall.

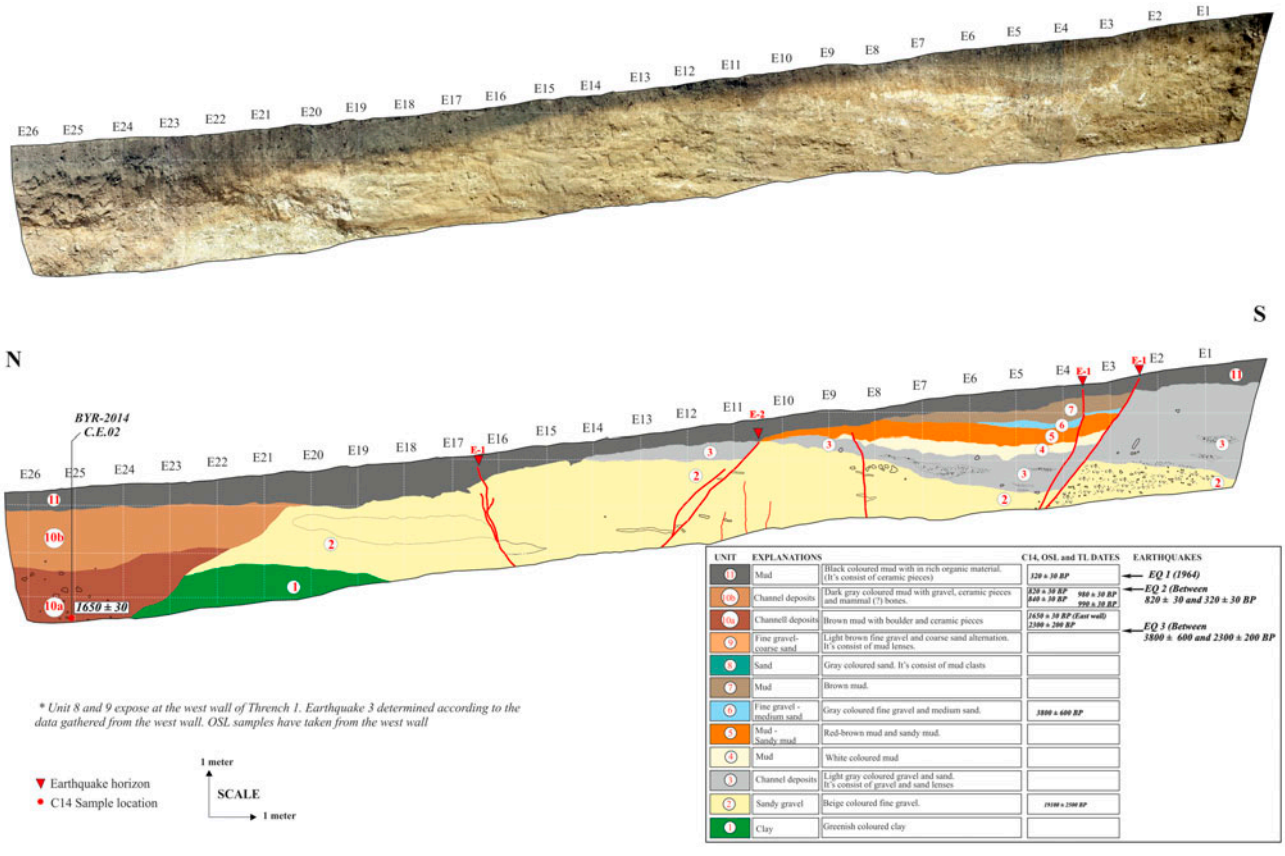

Figure 6. (a) Photomosaic of the Bayramiç Trench 1 eastern wall without interpretation and (b) Log of the Bayramiç Trench 1 eastern wall.

Formation consists of fluvial conglomerate, sandstone and lacustrine claystone in addition to, clayey limestone. The Mudamköy volcanic member is represented by andesite, dacite, basalt, tuff and agglomerate (Pehlivan et al., 2011). The Göbel Formation and Mudamköy volcanite member are exposed in the vicinity of the Eşen segment (Figure 3).

These units are unconformably covered by the Pliocene Bayramiç Formation, which is characterised by the alternation of fluvial conglomerate, sandstone, claystone and siltstone. It is exposed around the Dereköy and Salur segment.

Quaternary deposits are classified into eight primary units, described as lake and flood deposits of Lake Manyas (Q11 and Q12), old fluvial deposits (Q1), deltaic deposits (Qd), alluvial fan deposits (Qf), flood plain deposits (Qfp), undifferentiated alluvium (Qal) and modern fluvial deposits (Qa) (Figure 3).

2.3. The segment characteristics of the Manyas fault zone (MFZ) and its relation to the North Anatolian fault system

The Southern Marmara Region is primarily deformed by the active dextral strike-slip and normal faults belonging to the southern branch of the NAFS. The Yenice Gönen Fault and MFZ are active fault segments within the southern branch of the NAFS in the Southern Marmara Region. Both the 1953 Yenice Gönen earthquake (Ms = 7.2) and the 1964 Manyas earthquake (Ms = 6.9) were produced by these active faults. A 1-km-long part of the surface ruptures that occurred during both the

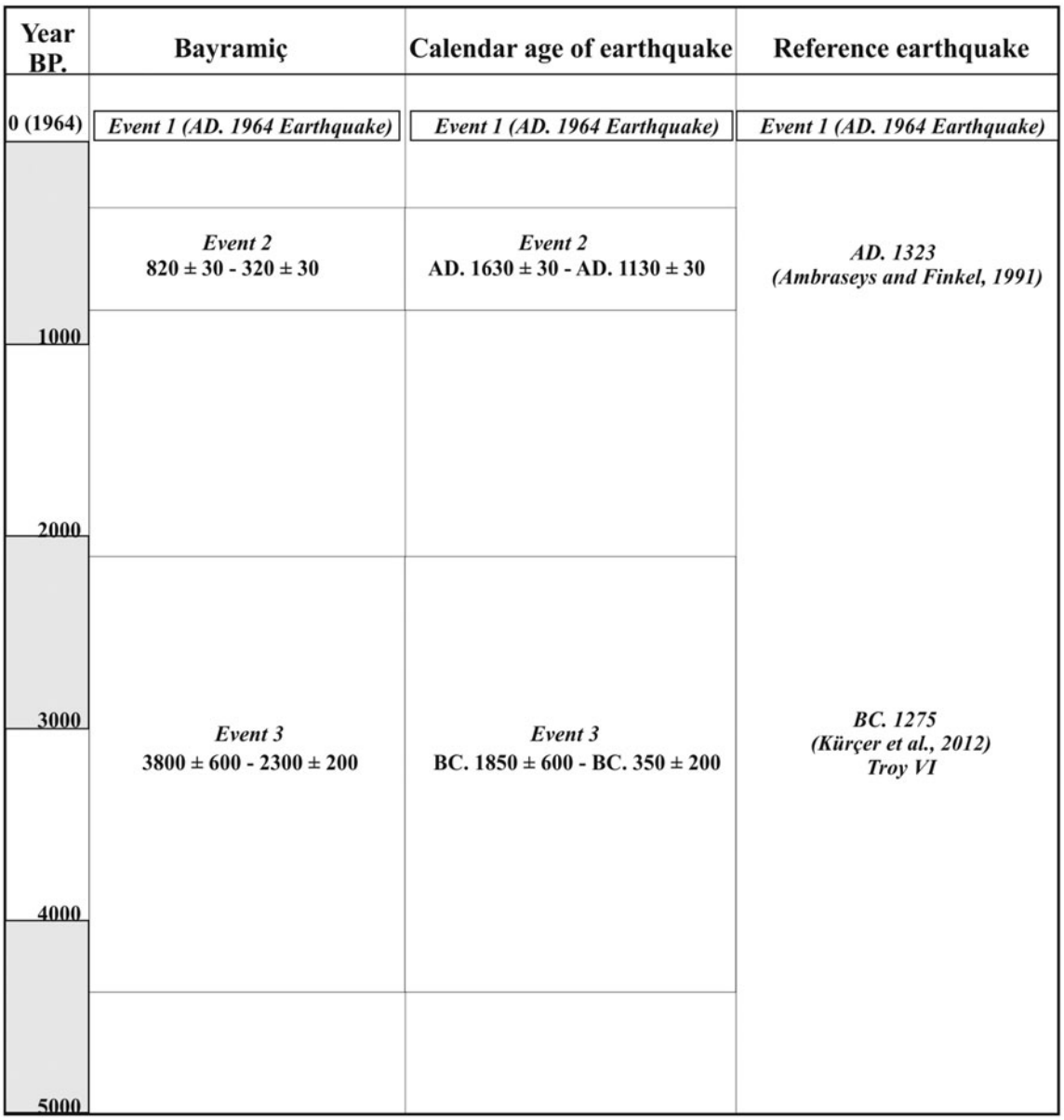

Figure 7. Interpretation of the earthquakes derived from the Bayramiç Trench Site.

Yenice Gönen and Manyas earthquakes overlapped each other. The NE-trending Yenice Gönen Fault and WNW–ESE-trending MFZ present a horse tail structure in the Southern Marmara Region (Figure 4).

The MFZ is a 38-km-long normal fault zone that extends in the WNW–ESE direction between the Yenice Gönen Fault to the west and the Mustafa Kemal Paşa fault to the east. The MFZ consists of three en-echelon geometric fault segments, named Dereköy, Salur and Eşen from SW to NE (Figure 3).

The 1964 Manyas earthquake caused surface deformation around the western part of the Dereköy and Salur segments. The Salur segment is a 16-km-long, WNW-trending normal fault segment that extends between Bayramiç in the west and Bölceağaç in the east. In this area, the Salur segment cuts the Bayramiç Formation and Quaternary deposits (Figure 3).

3. Paleoseismic trenching along the Manyas fault zone (MFZ)

In this study, paleoseismic trenching was performed in two different locations, named the Bayramiç and Hamamlı trench sites. The Bayramiç trench site is located to the west of the Salur segment (UTM Coordinates: 569807 E, 4440636 N) (Figure 3). The Hamamlı trench site is situated north of the Salur segment (NE of Hamamlı village) (GPS Coordinates: 35 0578972 E, 4440811 N) (Figure 3). In this locality, an observation pit was excavated to understand the surface deformation pattern documented by Erentöz and Kurtman (1964) and Ketin (1969).

Six charcoal, organic sediment and bone samples gathered from the Bayramiç trench site were dated at Beta Analytical Laboratories (USA) (Table 3). Additionally, two Optically Stimulated Luminescence (OSL) samples and two Thermo Luminescence (TL) samples were analysed in the Luminescence Dating Research Laboratory of Ankara University (Turkey) (Table 4). Trench walls were logged with a photomosaic technique using GIS software.

3.1. Bayramiç Trench site

Bayramiç Trenches were excavated on old fluvial deposits (Q1) (Figure 3). The fault trace is characteristic with a several-hundred-meter long linear fault scarp. Bayramiç trenches were excavated on local depressions formed by back-tilting.

Three trenches parallel to each other were excavated across to the Salur segment. They were named Bayramiç Trench 1, 2 and 3 (Figure 3). Bayramiç Trench 1 is 26 m-long, 3 m-deep and 5 m-wide, Bayramiç Trench 2 is 14 m-long, 3 m-deep and 4 m-wide and Bayramiç Trench 3 is 26 m-long, 3 m-deep and 5 m-wide.

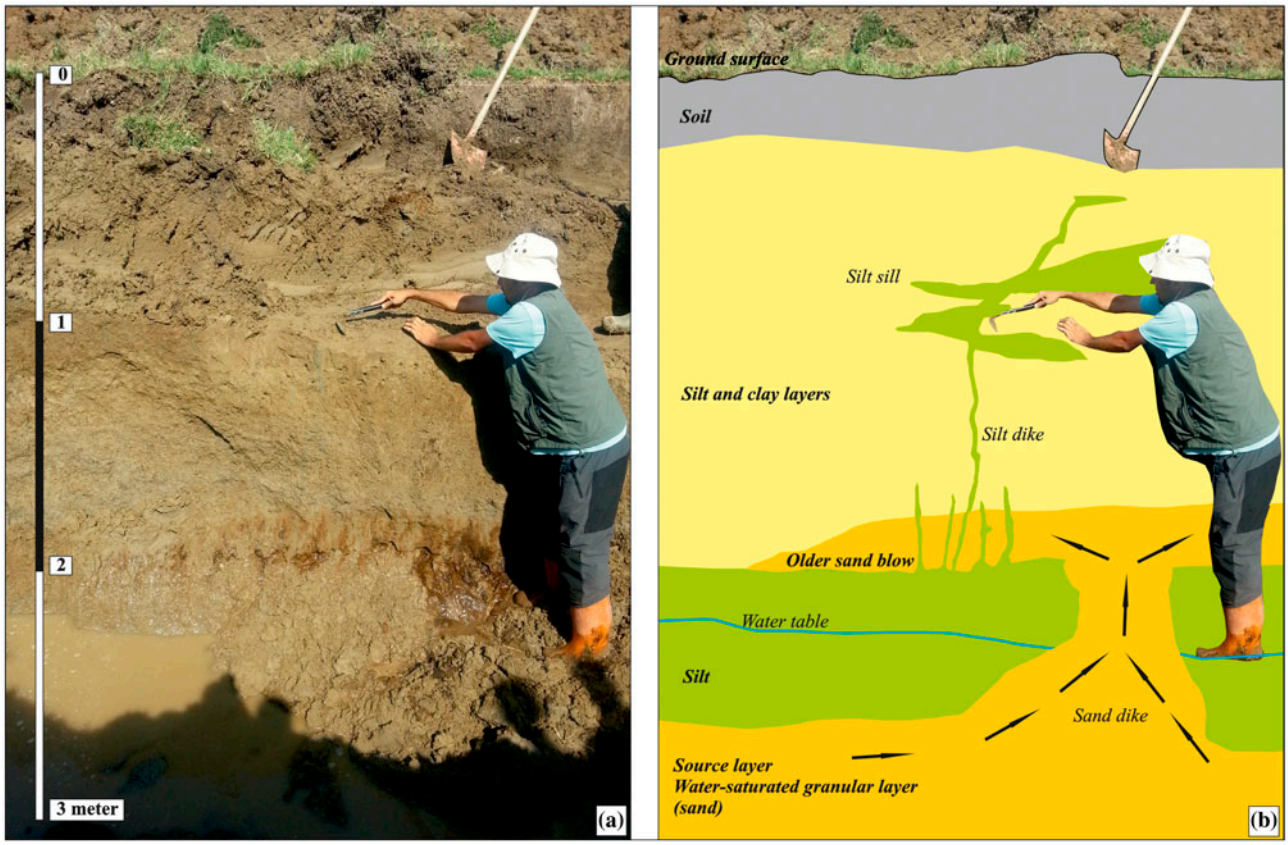

Figure 8. (a) Field photo and (b) Interpreted log of the Hamamlı Trench.

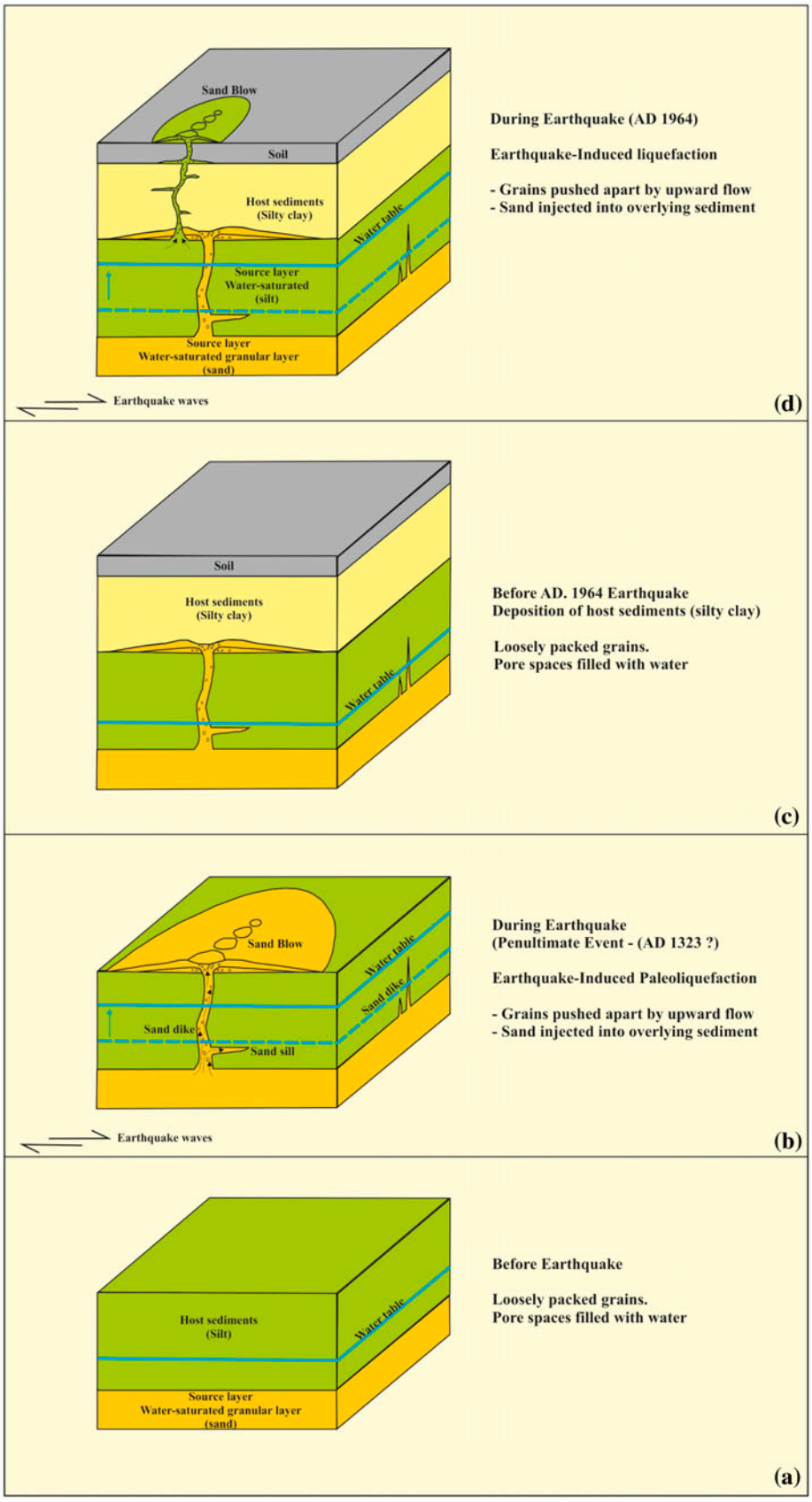

Figure 9. Schematic cross-section illustrating earthquake-induced liquefaction and formation of sand/silt dikes, sand/silt sills and sand blows (modified from Sims & Garvin, 1995).

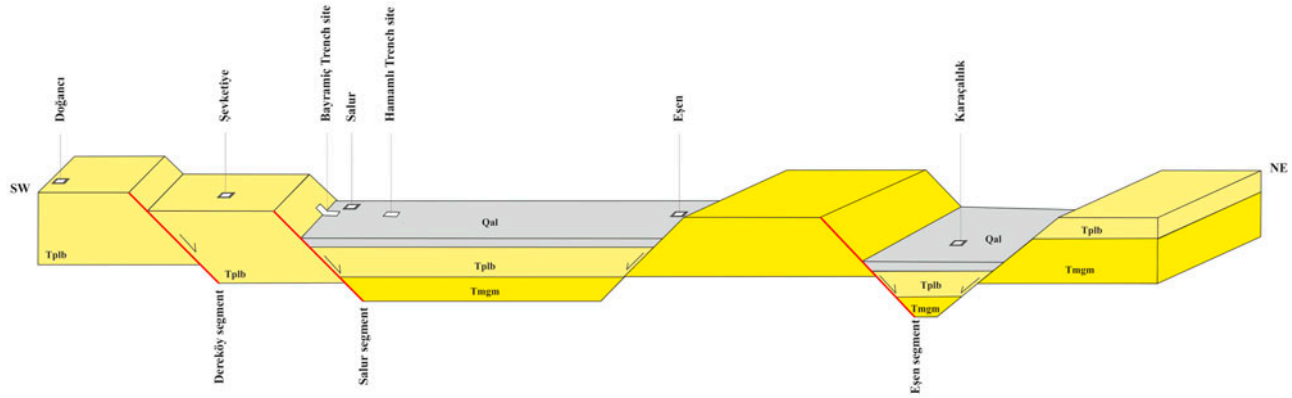

Figure 10. Block diagram showing the structural features of the Manyas fault zone.

Table 5. Fault plane slip data colected from Bayramiç Trench I and II.

Trench wall	Strike	Dip angle (°)	Dip direction	Rake	Fault type
Bayramiç Trench II / West wall	N 80° E	71°	NW	90° N	Normal
Bayramiç Trench II / West wall	N 85° E	67°	NW	90° N	Normal
Bayramiç Trench II / East wall	N 55° E	74°	NW	90° N	Normal
Bayramiç Trench II / East wall	N 65° E	58°	NW	60° N	Normal fault with sinistral strike-slip component
Bayramiç Trench III / West wall	N 73° W	69°	NE	90° N	Normal
Bayramiç Trench III / East wall	N 60° W	56°	SW	90° W	Normal
Bayramiç Trench III / East wall	N 80° W	64°	NE	90° N	Normal
Bayramiç Trench III / East wall	N 36° W	59°	SW	90° B	Normal
Bayramiç Trench III / East wall	N 50° W	74°	NE	90°	Normal

Table 6. Earthquake parameters proposed by different researchers regarding the Manyas earthquake.

Coordinates Lat.(°N)	Lon. (°E)	Location	Focal depth (km)	Faulting type	References
40.10	27.90	1.5 km SW of Hamamlı village (South of Salur segment)	24	Revers fault	Öcal et al. (1968)
–	–	–	–	Right lateral strike-slip fault	Ketin (1969)
40.30	28.23	18 km NE of Manyas Lake	10–20	Normal fault	McKenzie (1972)
40.18	28.12	5 km E of Manyas Lake		Oblique slip normal fault	Kıyak (1986)
–	–	–	–	Right lateral strike-slip fault	Şaroğlu et al. (1987)
40.30	28.20	16 km NE of Manyas Lake	–	–	Eyidoğan (1988)
40.30	28.23	18 km NE of Manyas Lake	14 ± 2	Normal fault	Taymaz et al. (1991)
40.10	28.00	3.6 km NE of Bölceağaç village	–	–	Ambraseys and Finkel (1991)
40.00	28.00	6 km SE of Manyas	–	–	Ambraseys and Jackson (1998)
40.10	28.20	12.8 km ESE of Manyas Lake	–	–	Ambraseys and Jackson (2000)
–	–	–	–	Right lateral strike-slip fault with normal component	Kürçer et al. (2015)

Whereas the paleoseismological results were obtained from Bayramiç Trench 1, fault plane slip data were collected and interpreted from the other two trenches. Three different stratigraphic packages were identified at Bayramiç Trenches 1 and 2. The oldest units are Late Pleistocene-Holocene fluvial sediments (Figure 5, Unit 1 – 9). This sequence was incised by late Holocene fluvial channel deposits comprising shards (Figures 5 and 6, Unit 10a and 10b). All of these units are unconformably overlain by modern soil (Figures 5 and 6, Unit 11).

Based on paleoseismological criteria such as stratigraphic and structural relations and upwards termination of fault strands, at least three events in the last 4000 years that resulted in a surface rupture, including

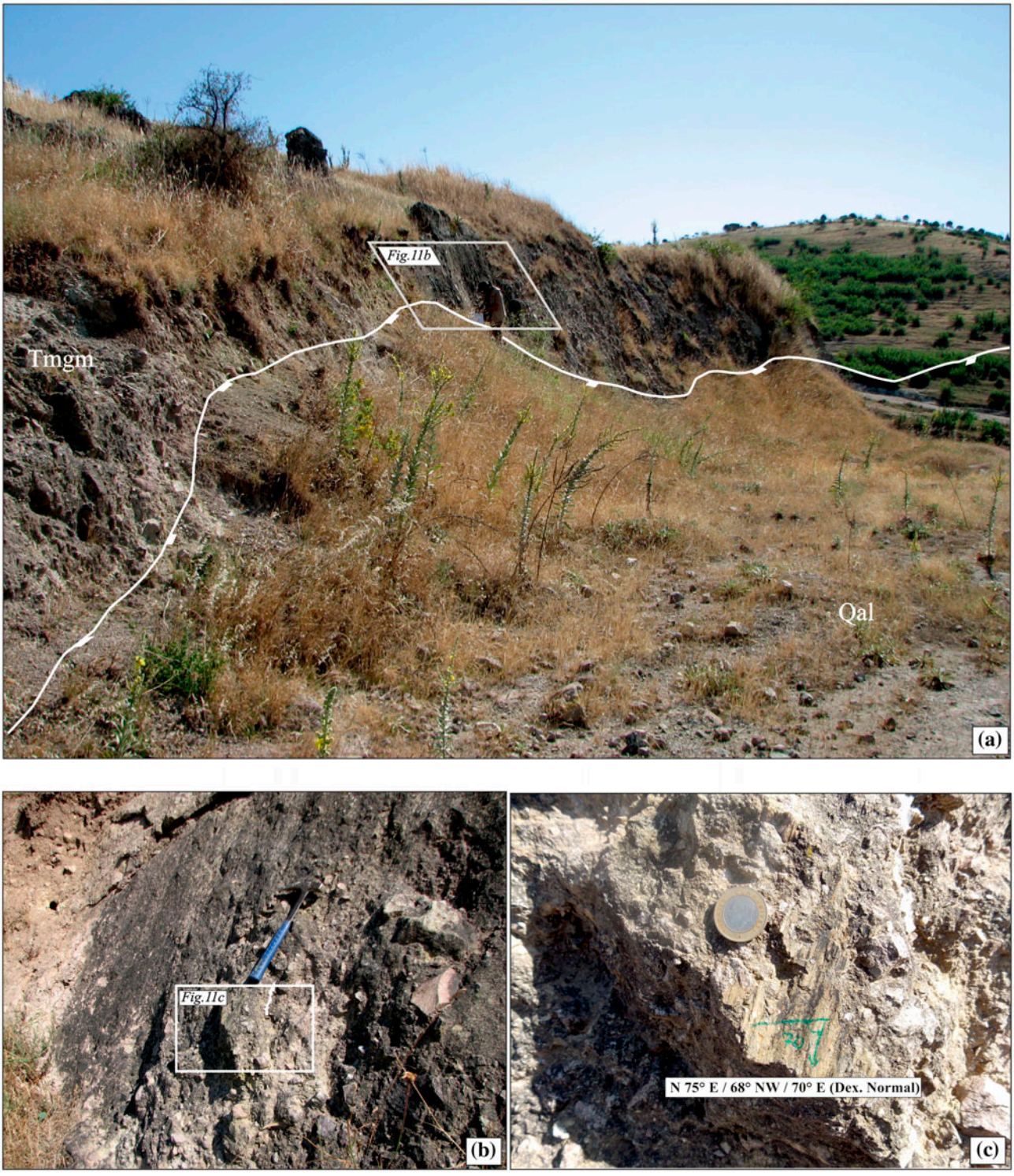

Figure 11. Fault plane slip data from Eşen segment of the Manyas fault zone near the Eşen village.

the 1964 earthquake were identified and dated at Bayramiç trenches.

Event 3

Event 3 is well identified between 21 and 22 meters in the west wall of Bayramiç Trench 1 (Figure 5). The earthquake horizon for this event was identified as the base of Unit 10a because Unit 2 was cut by the fault and covered by Unit 10a. Based on the OSL method, Unit 2 was dated to 19100 ± 2500 BP years. The radiocarbon age of Unit 10a is 2300 ± 200 BP. Because approximately 17 000 years of the sediment package (Units between 3 and 9) were eroded by fluvial channel Unit 10a, the age of Event 3 is unclear.

Event 2

Event 2 can be seen in both walls of Bayramiç trench 1 (Figure 5 and 6). Because the upward termination of the fault strand is covered by Unit 11, the earthquake horizon is defined as the base of Unit 11. The youngest radiocarbon age, obtained from Unit 10b below the earthquake horizon, is 820 ± 30 BP. The age of Unit 11 covering the earthquake horizon is dated to 320 ± 30 BP. According to these data, Event 2 should have occurred between 820 ± 30 BP and 320 ± 30 BP. Based on historical records, earthquakes occurred in both 1323 AD and 1556 AD (Ambraseys & Finkel, 1991) (Figure 2). Because of the epicenteral location of the 1323 AD earthquake, Event 2 seems to be associated with the MFZ. Therefore, Event 2 could be correlated with the 1323 AD earthquake.

Event 1 (6 October 1964. Manyas Earthquake – Ms=6.9)

The 1964 earthquake surface rupture is clearly seen on Bayramiç trench walls and is represented by normal fault characteristics in a narrow deformation zone between 2 and 4 mtrs on the east and west walls of Bayramiç Trench 1 (Figures 5 and 6). The age of Unit 11 is 320 ± 30 BP, which is the youngest unit. Because this unit is cut by a fault, this fault is interpreted as a 1964

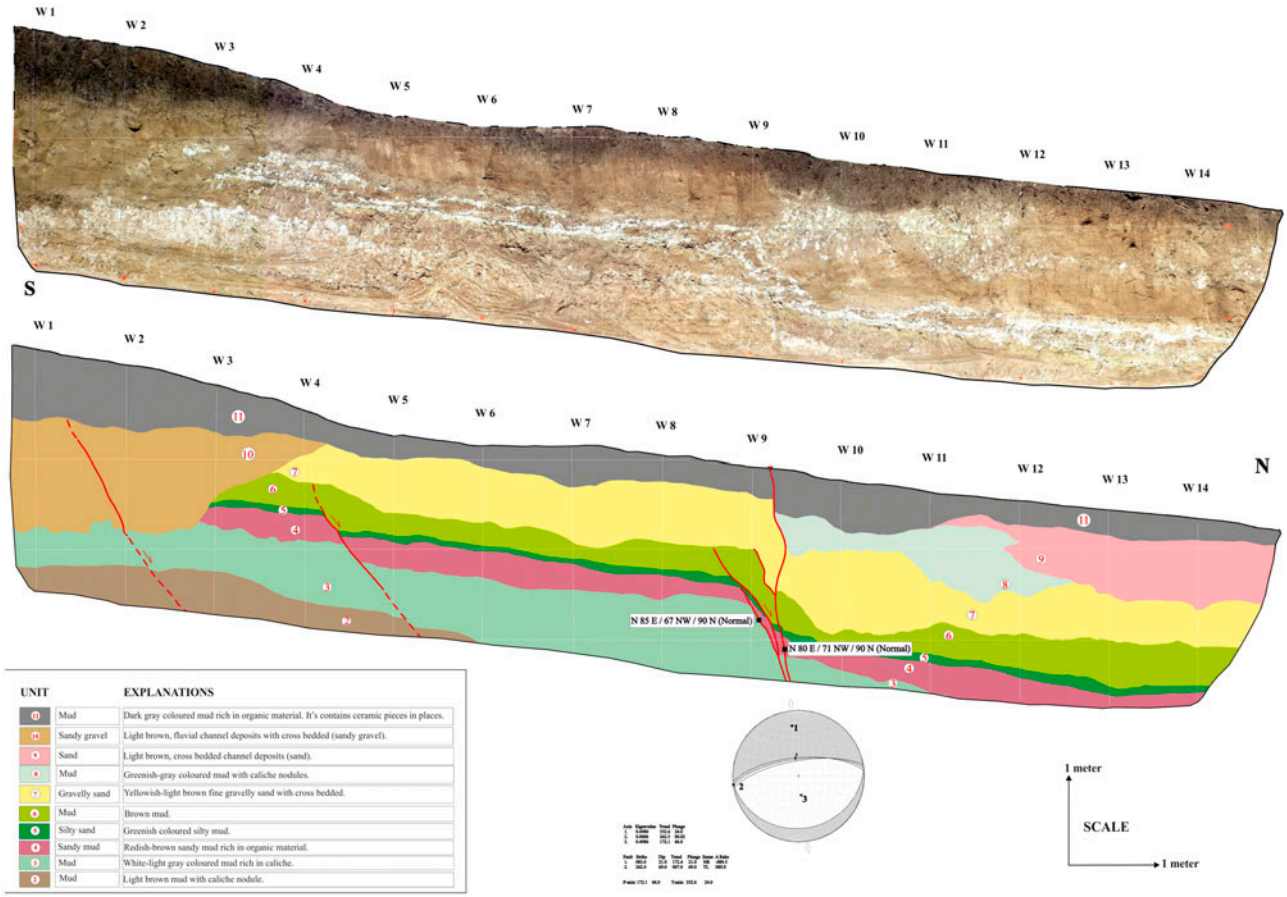

Figure 12. (a) Photomosaic of the Bayramiç Trench 2 western wall without interpretation and (b) Log of the Bayramiç Trench 2 western wall.
Equal-angle lower-hemisphere plots of fault slip data collected from the trenches. Fault and striae are superposed on a fault plane solution derived using the FaultKin program (Allmendinger, Cardozo, & Fisher, 2012; Marrett & Allmendinger, 1990; V 6.6.3). Arrows show tensional axis.

surface rupture. An interpretation of the earthquakes identified from Bayramiç Trenches is presented in (Figure 7).

3.2. *Hamamlı Trench site*

The most intensive surface deformation occurred around the Salur segment during the 1964 earthquake. However, the features of the surface deformation, particularly between the villages of Salur and Hamamlı are controversial. Erentöz and Kurtman (1964) suggested that the fractures occurred due to liquefaction and/or lateral spreading. Conversely, Ketin (1969) interpreted the NW–SE trending fractures as tension cracks resulting from, dextral strike-slip faulting.

We excavated a cross trench to the northeast of Hamamlı village (GPS Coordinates: 35 0578972 E, 4440811 N) to understand the origin of these surface deformational features (Figure 3).

The Hamamlı Trench site is located on the flood plain of the Manyas River (Qfp) (Figure 3). The groundwater table lies approximately 2 m below the surface. According to trench microstratigraphy, there is yellowish, water-saturated, fine sand at the bottom (approx. −4 m) Just above this unit, there is a yellowish-green, water-saturated, fine sand and silt alternation. Above the fine sand and silt alternation, there is yellowish clay, which is relatively more plastic. The recent soil level covers all of the units (Figure 8).

The crosscutting paleoliquefaction structures were observed at Hamamlı Trench (Figure 8). The model of earthquake-induced paleoliquefaction structures is illustrated in Figure 9.

The relatively older sand blow determined in Hamamlı Trench at −2 m is interpreted as a paleoliquefaction structure related to the penultimate event of 1964 earthquake. This event can be correlated with the 1323 AD earthquake.

4. Kinematic features of the Manyas fault zone (MFZ)

The MFZ consists of WNW–ESE-trending and northward-dipping normal faults. The general structural features of the fault zone are presented in Figure 10.

Kinematic data of the MFZ are limited. We were able to collect fault plane slip-data of the Eşen segment approximately 1.5 km northeast of the Eşen Village

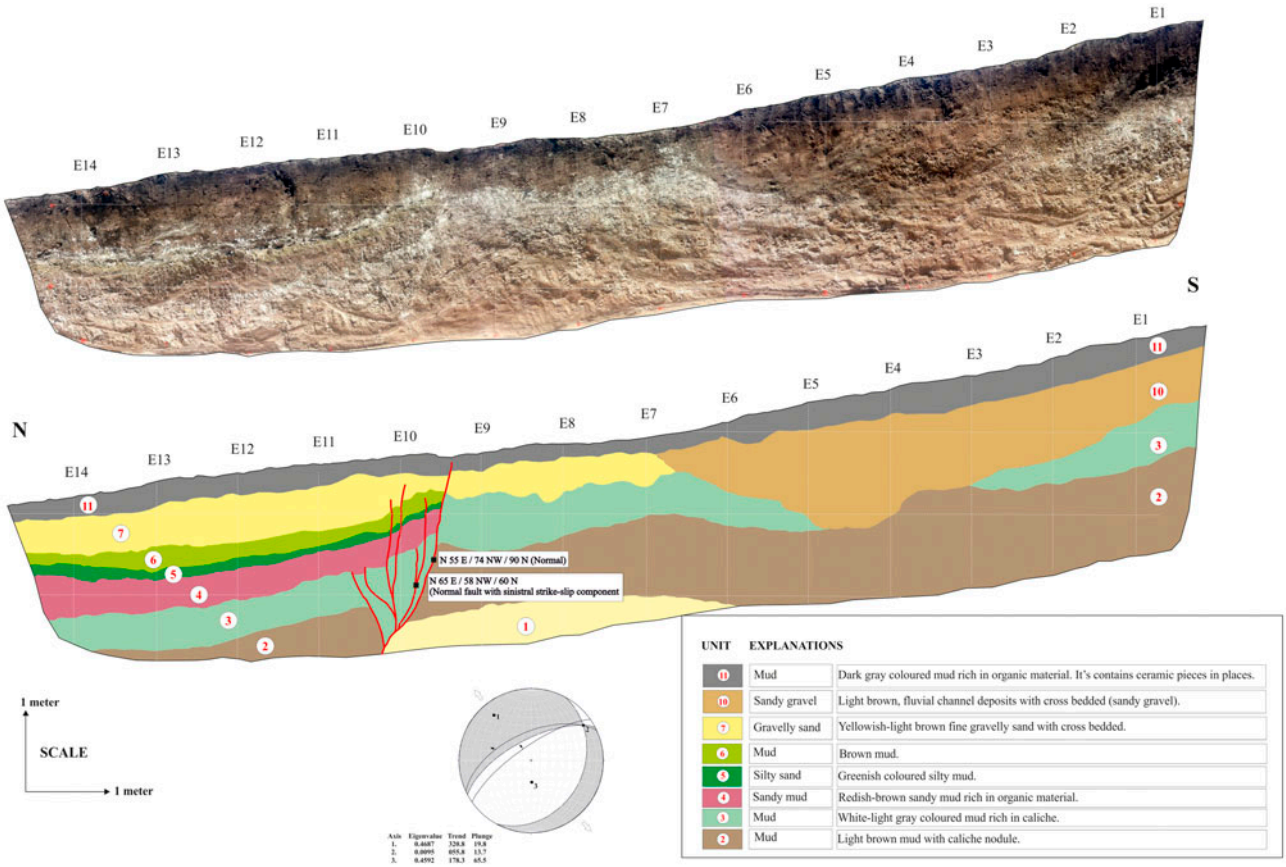

Figure 13. (a) Photomosaic of the Bayramiç Trench 2 eastern wall without interpretation and (b) Log of the Bayramiç Trench 2 eastern wall.
Equal-angle lower-hemisphere plots of fault slip data collected from the trenches. Fault and striae are superposed on a fault plane solution derived using the FaultKin program (Allmendinger et al., 2012; Marrett & Allmendinger, 1990; V 6.6.3). Arrows show tensional axis.

(Figure 11). According to the fault plane slip-data, the Eşen segment is a normal fault with a minor dextral strike-slip component.

The structural data, which reveals the recent kinematic features of the MFZ, was gathered from Bayramiç Trenches 2 and 3 (Table 5; Figures 12–15). According to the fault plane slip-data measured from the trench walls, the MFZ is a pure normal fault trending WNW–ESE and dipping 65°–75° towards to north.

5. Discussion and conclusion

The deformation of the Southern Marmara region is primarily controlled by the westernmost segments of the NAFS. To the east of Adapazarı, the NAFS splits into two main branches that extend towards the Marmara Sea and the Southern Marmara Region, forming a horse-tail structure (Barka, 1992; Barka & Gülen, 1988) (Figure 2). The northern and southern branches of the NAFS form an approximately 100-km-wide dextral shear zone in noertwestern Turkey (Figure 4). This shear zone is bordered by the Ganos and Saros segments to the north and the Havran-Balıkesir fault zone (HBFZ) (Sözbilir, Özkaymak, et al., 2016) and Edremit Fault Zone (EFZ) (Sözbilir, Sümer, et al., 2016) to the south (Figure 4).

The southern branch of the NAFS consists of several dextral strike-slip faults (e.g. the Yenice Gönen Fault and Sarıköy Fault), reverse faults (e.g. the Bekten fault; Özalp, Kürçer, Özdemir, & Duman, 2016) and normal faults (e.g. the Manyas Fault Zone and Uluabat Fault) associated with the dextral strike-slip faulting mechanism in the area of study. The 1944, 1953 and 1964 earthquakes were produced by the EFZ, YGF and MFZ, respectively (Figure 4).

The YGF is one of the most active dextral strike-slip faults in the Southern Marmara Region. A 70-km-long surface rupture occurred between Yenice and Gönen during the 18 March 1953, Yenice Gönen earthquake (Mw = 7.2). Eleven years after the Yenice Gönen earthquake, the Manyas earthquake (Ms = 6.9) occurred along the MFZ, on 6 October 1964. An 18-km-long surface rupture occurred as a result of the 1964 event along the Dereköy and Salur segments of the MFZ. 1-km-long part of surface rupture that was occurred both during the Yenice Gönen and Manyas earthquakes overlapped each other.

The MFZ is a WNW–ESE-trending 38-km-long normal fault zone that consists of three en-echelon fault segments, named Dereköy, Salur and Eşen from SW to NE. The MFZ is interpreted as a normal fault zone associated with dextral

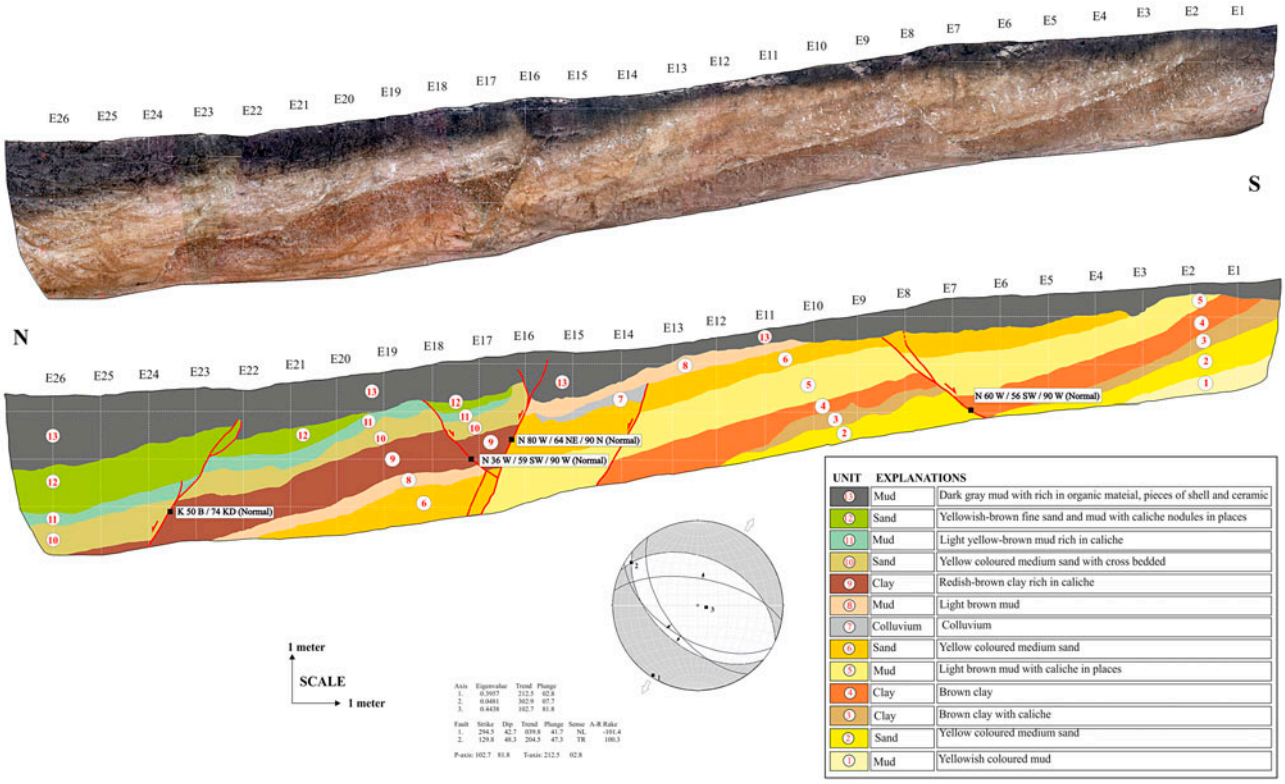

Figure 14. (a) Photomosaic of the Bayramiç Trench 3 eastern wall without interpretation and (b) Log of Bayramiç Trench 3 eastern wall.
Equal-angle lower-hemisphere plots of fault slip data collected from the trenches. Fault and striae are superposed on a fault plane solution derived using the FaultKin program (V 6.6.3, Allmendinger et al., 2012; Marrett & Allmendinger, 1990). Arrows show tensional axis.



Figure 15. Fault plane slip data collected from the Bayramiç Trench 2 and 3.

strike-slip faulting (see Figure 4). The NE-trending YGF and WNW–ESE-trending MFZ presents as horse-tail structure in the Southern Marmara region (Figure 4).

On 6 October 1954, an earthquake (Ms = 6.9) occurred along the MFZ. Although some surface deformation occurred around the Salur segment, there is

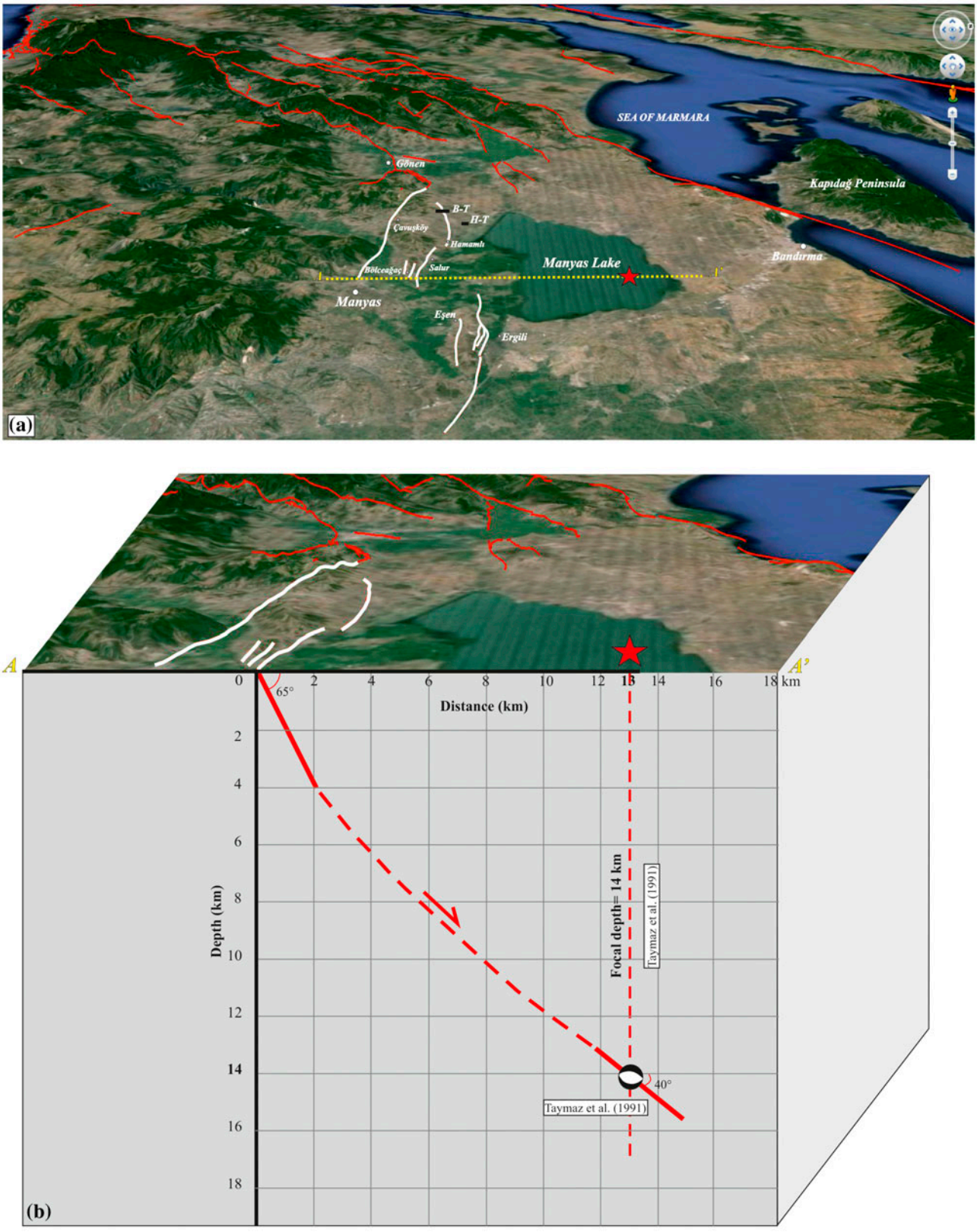

Figure 16. Seismotectonic model diagram regarding Manyas earthquake (a) Google image of the Manyas fault zone and (b) schematic block diagram.

no record of surface faulting. The characteristics of the surface deformation during the Manyas earthquake and the seismotectonic features of the source fault are controversial.

In this study, paleoseismologic trench studies performed on the Salur segment of the MFZ resulted in the gathering of new and substantial data to overcome the discussions outlined above. At least three large earthquakes within the last 4000 years that resulted in surface ruptures, including the 1964 earthquake, have been identified and dated.

The penultimate event (before the 1964 earthquake) was dated to between 820 ± 30 BP and 320 ± 30 BP and attributed to the 1323 AD earthquake (Ambraseys & Finkel, 1991).

The ante-penultimate event was dated to between 3800 ± 600 BP and 2300 ± 200 BP, but there are no archaeological data or historical records associated with this earthquake.

To understand the origin of the surface deformations that occurred during the Manyas earthquake along the Salur segment a trench was excavated to the north of Hamamlı village. Paleoliquefaction structures crossing each other were observed in the Hamamlı trench. We concluded that the surface deformations that occurred during the 1964 earthquake are primarily the consequence of liquefaction.

Based on the fault plane slip-data, the MFZ is a purely normal fault that trends WNW–ESE and dips 64°–74° to the NNE. The Eşen segment of the fault zone has a minor dextral strike-slip component.

The seismotectonic features of the 1964 Manyas earthquake (Ms = 6.9) are controversial in the literature. There are substantially different views about the epicenter, focal depth and the faulting type of the earthquake.

We suggest a new seismotectonic model for the Manyas earthquake (Figure 16). In this model, a surface rupture is assumed to have occurred along the Salur segment of the MFZ during the Manyas earthquake. Fault plane slip-data collected from Bayramiç Trenches show that the MFZ is a purely normal fault trending to the WNW–ESE and dipping 64°–74° NNE (Table 5). We assume that the focal depth of the Manyas earthquake was 14 ± 2 km and that the dip of the fault plane at the hypocenter was 40° NNE (Taymaz et al., 1991).

According to these data, the MFZ should have a listric geometry. The epicentral location for the Manyas earthquake should be somewhere within Manyas Lake (Figure 16).

Because of the local geological conditions and the proximity of the epicentre, the surface deformations, including liquefaction and lateral spreading, are concentrated between the villages of Salur and Hamamlı.

Acknowledgements

This work has been realised in the frame of the Paleoseismological Researches Project of Turkey (TURKPAP). Grant No: 2013-30-14-07. Financial support has been provided by the General Directorate of Mineral Research and Exploration of Turkey (MTA). We are grateful to Özgül Sönmez (MTA) for her assistance during the study. We are thankful to all organisations and executives for their supports. We would like to thank sincerely to Prof. Dr. Hasan Sözbilir (Dokuz Eylül University) and anonymous referee whose valuable comments and useful criticisms have greatly improved the manuscript.

Disclosure statement

No potential conflict of interest was reported by the authors.

Funding

This work was financially supported by the General Directorate of Mineral Research and Exploration of Turkey (MTA) [grant number 2013-30-14-07].

ORCID

Akın Kürçer http://orcid.org/0000-0001-8646-5113
Selim Özalp http://orcid.org/0000-0002-6755-4206

References

Akçay, A. E., Dönmez, M., Ilgar, A., Duru, M., & Pehlivan, P. (2008). *1:100 000 scale geological map series of Turkey, Bandırma (H 19) Quadrangle*. Ankara: General Directorate of Mineral Research and Exploration.

Aktuğ, B., Nocquet, J. M., Cingöz, A., Parsons, B., Erkan, Y., England, P., … Tekgül, A. (2009). Deformation of western Turkey from a combination of permanent and campaign GPS data: Limits to block-like behavior. *Journal of Geophysical Research, 114*, B10404. doi:10.1029/2008JB006000

Allmendinger, R. W., Cardozo, N., & Fisher, D. (2012). *Structural geology algorithms: Vectors and tensors in structural geology*. Cambridge: Cambridge University Press, 302.

Ambraseys, N. (1988). Engineering seismology. *Earthquake engineering and structural dynamics, 17*, 1–105.

Ambraseys, N. N. (2002). The seismic activity of the Marmara Sea region over the last 2000 years. *Bulletin of the Seismological Society of America, 92*(1), 1–18.

Ambraseys, N., & Finkel, C. F. (1991). Long-term seismicity of İstanbul and of the Marmara sea region. *Terra Nova, 3*, 527–539.

Ambraseys, N., & Jackson, J. (1998). Historical recent earthquakes Eastern Mediterranean. *Geophysical Journal International, 133*, 390–406.

Ambraseys, N., & Jackson, J. (2000). Seismicity of the sea of Marmara (Turkey) since 1500. *Geophysical Journal International, 141*, F1–F6.

Armijo, R., Meyer, B., Hubert-Ferrari, A., & Barka, A. (1999). Westward propagation of North Anatolian fault into the Northern Aegean: Timing and kinematics. *Geology, 27*, 267–270.

Ayhan, A., Alsan, E., Sancaklı, N., & Üçer, S.B. (1981). *Türkiye ve Dolayları Deprem Kataloğu 1881–1980* [Earthquake Cataloque of Turkey and its vicinity 1881–1980]. İstanbul: Boğaziçi University, Kandilli Observatory, Publications of Seismology (in Turkish).

Barka, A. A. (1992). The North Anatolian fault zone. *Annales Tectonicae, 6*, 164–195.

Barka, A., & Gülen, L. (1988). New constrains on age and total offset on the North Anatolian fault zone: Implications for tectonics of the Eastern Mediterranean region. *METU Journal of Pure and Applied Sciences, 21*, 39–63.

Bozkurt, E. (2001). Neotectonics of Turkey – A synthesis. *Geodinamica Acta, 14*, 3–30.

Canıtez, N. (1968). Earthquake focal mechanisms and stress distributions of Turkey and its vicinity. *İ.T.Ü. Faculty of Mining* Assoc. Prof. Thesis (unpublished), İstanbul.

Canıtez, N. & Üçer, B. (1967). Computer determinations for the faultplane solutions in and near Anatolia. *Tectonophysics, 4*, 235–244.

Duman, T. Y., Çan, T., Emre, Ö., Kadiroğlu, F. T., Başarır Baştürk, N., Kılıç, T., … Kurt, A. İ. (2016). Seismotectonic database of Turkey. *Bulletin Earthquake Engineering*. doi:10.1007/s10518-016-9965-9

Duru, M., Pehlivan, Ş., Okay, A. İ., Şentürk, Y., & Kar, H. (2012). Biga Yarımadası'nın Tersiyer Öncesi Jeolojisi [Pretertiary geology of Biga Peninsula]. In E. Yüzer ve & G. Tünay (Eds.), *Biga Yarımadası'nın Genel ve Ekonomik Jeolojisi* [General and economical geology of Biga Peninsula] (Chapter, 1, pp. 7–74). Ankara: General Directorate of Mineral Research and Exploration. ISBN: 978-605-5310-18-9.

Emre, Ö., Kazancı, N., Erkal, T., Karabıyıkoğlu, M., & Kuşçu, İ. (1997). Uluabat ve Manyas Göllerinin Oluşumu ve Yerleşim Tarihçesi [Rapor Bölümü, Güney Marmara Bölgesinin Neojen-Kuvaterner Evrimi]. *Evolution and setting history of the Uluabat and Manyas Lakes* [Report Chapter of Neogene and Quaternary evolution of the Southern Marmara Region] (Chapter, 7, pp. 116–134). Tübitak, Ankara, Turkey.

Emre, Ö., Doğan, A., Özalp, S., & Yıldırım, C. (2011). *1:250 000 scale active fault map series of Turkey, Bandırma (NK 35-11b) Quadrangle*. Serial number: 3. Ankara: General Directorate of Mineral Research and Exploration.

Emre, Ö., Duman, T. Y., Özalp, S., Elmacı, H., Olgun, Ş., & Şaroğlu, Ş. (Eds.). (2013). *Active fault map of Turkey with explanatory text*. Ankara: General Directorate of Mineral Research and Exploration, Special Publication Series-30.

Erentöz, C., & Kurtman, F. (1964). 1964 yılı Manyas depremi üzerine rapor [The report on 1964 Manyas Earthquake]. *Bulletin of MTA, 63*, 1–5.

Ergintav, S., Reilinger, R. E., Çakmak, R., Floyd, M., Cakir, Z., Doğan, U., … Özener, H. (2014). Istanbul's earthquake hot spots: Geodetic constraints on strain accumulation along faults in the Marmara seismic gap. *Geophysical Research Letters, 41*, 5783–5788.

Eyidoğan, H. (1988). Rates of crustal deformation in western Turkey as deduced from major earthquakes. *Tectonophysics, 148*, 83–92.

Flerit, F., Armijo, R., King, G., & Meyer, B. (2004). The mechanical interaction between the propagating North Anatolian Fault and the back-arc extension in the Aegean. *Earth and Planetary Science Letters, 224*, 347–362.

Genç, Ş. C., Dönmez, M., Akçay, A. E., Altunkaynak, Ş., Eyüboğlu, M., & Ilgar, Y. (2012). Biga Yarımadası'nın Tersiyer Volkanizmasının Stratigrafik, Petrografik ve Kimyasal Özellikleri [Kitap bölümü, Biga Yarımadası'nın Genel ve Ekonomik Jeolojisi]. In E. Yüzer ve, G. Tünay (Eds.), *Stratigraphic, Petrographic and Chemical features of Tertiary Volcanism of Biga Peninsula* [Book chapter of General and Economical Geology of Biga Peninsula] (Chapter, 3, pp. 122–162). Ankara: General Directorate of Mineral Research and Exploration. ISBN: 978-605-5310-18-9.

Jackson, J., & McKenzie, D. P. (1984). Active tectonics of the Alpine-Himalayan Belt between western Turkey and Pakistan. *Geophysical Journal of the Royal Astronomical Society, 77*, 185–246.

Karakaisis, G. F., Papazachos, C. F., & Scordilis, E. M. (2010). Seismic sources and main seismic faults in the aegean and surrounding area, bulletin of the geological society of Greece. Proceedings of the 12th International Congress (pp. 2016–2042), Patras.

Ketin, I. (1969). Kuzey Anadolu Fayı hakkında [The North Anatolian fault]. *Bulletin of MTA, 72*, 1–25.

Kıyak, Ü., (1986). *Kuzey Anadolu Fay zonunun batı uzantılarının incelenmesi*. [Investigation of the western extensions of North Anatolian Fault] (Unpublished PhD. Thesis). xxiii, 214, İstanbul University Graduate School of Natural and Applied Sciences, İstanbul.

Kocaefe, S. & Ataman, G. (1976). Actual tectonics of the western Anatolia. *Yerbilimleri, 9*, 149–162.

Kürçer, A., Yalçın, H., Gülen, L., & Kalafat, D. (2015). 8 January 2013 Mw=5.7 North Aegean Sea Earthquake Sequence and its Seismotectonic Significance. *Geodinamica Acta, 27*, 175–188.

Le Pichon, X. N., Chamot-Rooke, S., Lallemant, R., Noomen, G., & Veis (1995). Geodetic determination of the kinematics of central Greece with respect to Europe implications for eastern Mediterranean tectonics. *Journal of Geophysical Research, 100*, 12675–12690.

Marrett, R. A., & Allmendinger, R. W. (1990). Kinematic analysis of fault-slip data. *Journal of Structural Geology, 12*, 973–986.

McClusky, S., Reilinger, R., Mahmoud, S., Ben Sari, D., & Tealeb, A. (2003). GPS constraints on Africa (Nubia) and Arabia plate motions. *Geophysical Journal International, 155*, 126–138.

McKenzie, D. P. (1972). Active tectonics of the Mediterranean region. *Geophysical Journal of the Royal Astronomical Society, 30*, 109–185.

McKenzie, D. P. (1978). Active tectonics of the Alpine Himalayan belt the Aegean Sea and surrounding regions. *Geophysical Journal of the Royal Astronomical Society, 55*, 217–254.

Meade, B. J., Hager, B. H., McClusky, S. C., Reilinger, R. E., Ergintav, S., Lenk, O., … Özener, H. (2002). Estimates of seismic potential in the Marmara region from block models of secular deformation constrained by GPS measurements. *Bulletin of the Seismological Society of America, 92*, 208–215.doi:

Öcal, N., Üçer, S. B., ve Taner, D. (1968). *Manyas-Karacabey depremi 6 Ekim 1964* [6 October 1964 Manyas Karacabey Earthquake]. (Vol. 11). İstanbul: Boğaziçi University, Kandilli Observatory, Publications of Seismology.

Örgülü, G. & Aktar, M. (2001). Regional moment tensor inversion for strong aftershocks of the August 17, 1999 İzmit earthquake (Mw= 7.4). *Geophys. Res. Lett., 28*, 371–74.

Özalp, S., Kürçer, A., Özdemir, E., & Duman, T. Y. (2016). The Bekten Fault: The palaeoseismic behavior and kinematic characteristics of an intervening segment of the North Anatolian fault zone, Southern Marmara Region, Turkey. *Geodinamica Acta, 28*, 347–362. doi:10.1080/09853111.2016.1208524

Papadopoulos, G. A., Kondopoulou, D. P., Leventakis, G. A., & Pavlides, S. B. (1986). Seismotectonics of the Aegean region. *Tectonophysics, 124*, 67–84.

Pehlivan, Ş., Duru, M., Kanar, F., & Kandemir, Ö. (2011). *1:100 000 Scale Geological Map Series of Turkey, Bandırma (H 20) Quadrangle*. Ankara: General Directorate of Mineral Research and Exploration.

Reilinger, R., McClusky, S., Vernant, P., Lawrence, S., Ergintav, S., Cakmak, R., … Karam, G. (2006). GPS constraints on continental deformation in the Africa-Arabia-Eurasia continental collision zone and implications for the dynamics of plate interactions. *Journal of Geophysical Research, 111*, B05411.

Şaroğlu, F., Emre, Ö., & Boray, A. (1987). *Türkiye'nin Diri Fayları ve Depremsellikleri* [Active faults of Turkey and their seismicity's] (MTA Report No: 8174, 394 s) Ankara.

Şengör, A. M. C. (1979). The North Anatolian transform fault: Its age, offset and tectonic significance. *Journal of the Geological Society, 136*, 269–282.

Şengör A. M. C. (1980). *Turkiye'nin Neotektoniği'nin Esasları* [The Fundamentals of Turkish Neotectonics]. Ankara: Publication of the geological society of Turkey 40s (in Turkish).

Şengör, A. M. C., & Barka, A. A. (1992). Evolution of escaperelated strike-slip systems: Implications for distribution of collisional orogens. 29th International Geological Congress, Kyoto, Japan, Abstracts, 1, 232.

Şengör, A. M. C., Görür, N., & Şaroğlu, F. (1985). Strike-slip faulting and related basin formation in zones of tectonic escape: Turkey as acase study. İn K. T. Biddle & N. Christie-Blick (Eds.), *Strike-slip faulting and basin formation* (Vol. 37, pp. 227–264). Tulsa, OK: Society of Economic Paleontologists and Mineralogists Special Publication.

Şengör, A. M. C., Tüysüz, O., İmren, C., Sakınç, M., Eyidoğan, H., Görür, N., & Rangin, C. (2004). The North Anatolian fault: A new look. *Annual Review of Earth and Planetary Sciences, 33*, 1–77. doi:10.1146/annure.earth.32.101802.120415

Sims, J. D., & Garvin, C. D. (1995). Recurrent liquefaction induced by the 1989 Loma Prieta earthquake and 1990 and 1991 aftershocks: Implications for paleoseismicity studies. *Bulletin of the Seismological Society of America, 85*, 51–65.

Sözbilir, H., Özkaymak, Ç., Uzel, B., Sümer, Ö., Eski, S., & Tepe, Ç. (2016). Palaeoseismology of the Havran-Balıkesir fault zone: Evidence for past earthquakes in the strike-slip-dominated contractional deformation along the southern branches of the North Anatolian fault in northwest Turkey. *Geodinamica Acta, 28*, 254–272. doi:10.1080/09853111.2016.1171111

Sözbilir, H., Sümer, Ö., Özkaymak, Ç., Uzel, B., Güler, T., & Eski, S. (2016). Kinematic analysis and palaeoseismology of the Edremit fault zone: Evidence for past earthquakes in the southern branch of the North Anatolian fault zone, Biga Peninsula, NW, Turkey. *Geodinamica Acta, 28*, 273–294. doi:10.1080/09853111.2016.1175294

Sylvester, A. G. (1988). Strike-slip faults. *Geological society of America Bulletin, 100*, 1666–1703. doi:10.1130/0016-7606(1988)100<1666:ssf>2.3.co;2

Taymaz, T., Jackson, J., & McKenzie, D. P. (1991). Active tectonics of the north and central Aegean Sea. *Geophysical Journal International, 106*, 433–490.